

Orbital Symmetry and Electron Correlation in Na_xCoO_2

W. B. Wu,^{1,2} D. J. Huang,^{1,2,*} J. Okamoto,¹ A. Tanaka,³ H.-J. Lin,¹ F. C. Chou,⁴ A. Fujimori,⁵ and C. T. Chen¹

¹National Synchrotron Radiation Research Center, Hsinchu 30077, Taiwan

²Department of Electrophysics, National Chiao-Tung University, Hsinchu 300, Taiwan

³Department of Quantum Matters, ADSM, Hiroshima University, Higashi-Hiroshima 739-8530, Japan

⁴Center for Materials Science and Engineering, Massachusetts Institute of Technology, Cambridge, MA 02139, U.S.A.

⁵Department of Complexity Science and Engineering, University of Tokyo, Chiba 277-8561, Japan

(Dated: March 23, 2022)

Measurements of polarization-dependent soft x-ray absorption reveal that the electronic states determining the low-energy excitations of Na_xCoO_2 have predominantly a_{1g} symmetry with significant O 2p character. A large transfer of spectral weight observed in O 1s x-ray absorption provides spectral evidence for strong electron correlations in the layered cobaltates. Comparing Co 2p x-ray absorption with calculations based on a cluster model, we conclude that Na_xCoO_2 exhibits a charge-transfer electronic character rather than a Mott-Hubbard character.

PACS numbers: 71.27.+a, 74.70.-b, 71.70.-d, 78.70.Dm

Sodium cobalt oxides (Na_xCoO_2) have attracted renewed interest because of their exceptionally large thermoelectric power [1] and the recent discovery of superconductivity in their hydrated counterparts [2]. Despite intensive experimental [1, 2, 3, 4, 5, 6, 7, 8, 9] and theoretical [10, 11, 12, 13, 14, 15, 16, 17, 18, 19] work, there remain many unresolved issues concerning the electronic structure of Na_xCoO_2 .

An important issue is the orbital character of the valence electrons responsible for low-energy excitations. The lattice of Na_xCoO_2 exhibits a trigonal distortion; its CoO_2 layer consists of a triangular net of distorted edge-sharing oxygen octahedra with Co at the center, leading to a splitting of t_{2g} states into e_g^π and a_{1g} states as shown in Fig. 1. The e_g^π states spread over the ab plane, whereas the a_{1g} state extends to the c -axis; in a coordination system in which the z -axis is along the c -axis, the a_{1g} state is $d_{3z^2-r^2}$ and the two e_g^π states are $\frac{1}{\sqrt{3}}(d_{yz} + \sqrt{2}d_{xy})$ and $\frac{1}{\sqrt{3}}(d_{zx} - \sqrt{2}d_{x^2-y^2})$. Band-structure calculations in the local-density approximation (LDA) show that the a_{1g} state at the Γ point has a one-particle energy of 1.6 eV higher than that of the e_g^π states [10]. Thereby, the e_g^π states are almost filled, while the a_{1g} is partially filled and is the electronic state most relevant to low-energy excitations. These calculations are however different from a viewpoint based on a crystal-field approach. According to a point-charge model, one would expect that the compressed trigonal distortion stabilizes the a_{1g} state with an energy ~ 0.025 eV lower than that of e_g^π [12], as illustrated in Fig. 1(B).

To comprehend the effect of electron correlations and the trigonal distortion on t_{2g} states are imperative for an understanding of the electronic structure of Na_xCoO_2 . One requires spectral evidence for electron correlations to justify a microscopic model of correlated electrons to explain the spectacular physical properties of Na_xCoO_2 . Based on the LDA results [10] that the a_{1g} band is separated from the e_g^π bands, authors of several theoretical

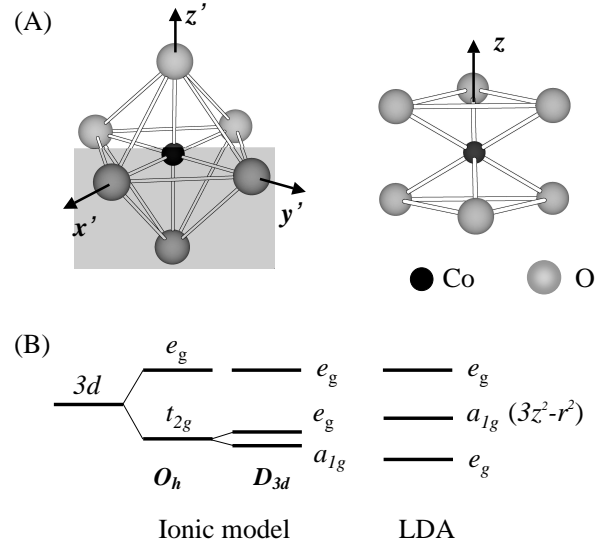


FIG. 1: (A) Illustration of the trigonal distortion of a CoO_6 octahedron. Left panel: undistorted CoO_6 octahedron with cubic (O_h) symmetry. Right panel: compressed CoO_6 octahedron with D_{3d} symmetry. The distorted CoO_6 is rotated such that the three-fold rotation axis is along the c -axis. (B) Crystal-field splitting of Co 3d states in distorted CoO_6 according to an ionic model and relative energy positions of 3d bands obtained from LDA calculations.

works have proposed one-band models for the superconductivity, such as the extended Hubbard model [13] and the $t - J$ model based on the resonating valence bond (RVB) theory [14, 15, 16]. In contrast, multi-band models [12, 17] were also proposed for the triangular cobaltates. Thus evidence for electron correlations and the validity of one-band models are fundamental questions for the underlying physics of Na_xCoO_2 .

Another primary issue is whether the electronic states of $\text{Na}_{0.5}\text{CoO}_2$ responsible for low-energy excitations have O 2p character. Early LDA calculations [10] indicate that

hybridization between Co 3*d* and O 2*p* in Na_{0.5}CoO₂ is weak. Analysis of core-level photoemission results suggests that Na_{*x*}CoO₂ has a Mott-Hubbard-like rather than a charge-transfer electronic structure [6]. On the other hand, recent LDA results corroborated with a Hubbard-like model conclude that Na_{1/3}CoO₂ exhibits significant hybridization between Co 3*d* and O 2*p* states [18].

In this Letter, we present measurements of soft x-ray absorption spectra (XAS) on Na_{*x*}CoO₂ pertinent to its electronic structure such as orbital character of the electronic states determining the low-energy physics. In addition, we discuss the spectral character of strongly correlated electrons in a one-electron addition process. Comparison of O 1*s* XAS with various doping shows that Co 3*d* electrons are strongly correlated. To investigate the detailed electronic structure, we compared Co 2*p* XAS with results of calculations using a cluster model in the configuration-interaction (CI) approach.

Single crystals of Na_{0.75}CoO₂ were grown by the traveling solvent floating-zone method. Crystals with smaller Na concentrations of *x* = 0.67 and 0.5 were prepared from Na_{0.75}CoO₂ through subsequent electrochemical de-intercalation procedures, as confirmed by Electron Microprobe Analysis. Details of crystal growth, electrochemical de-intercalation, and characterization of the resulting samples are discussed elsewhere [20].

We measured XAS on Na_{*x*}CoO₂ single crystals using the Dragon beamline at the National Synchrotron Radiation Research Center in Taiwan. The XAS were recorded through collecting the sample drain current. Crystals were freshly cleaved in ultra-high vacuum with a pressure lower than 5×10^{-10} torr at 80 K. The incident angle was 60° from the sample surface normal; the photon energy resolutions were set at 0.12 eV and 0.25 eV for photon energies of 530 eV and 780 eV, respectively. In polarization-dependent measurements, we rotated the sample about the direction of incident photons to obtain XAS from which experimental artifacts related to the difference in the optical path and to the probing area have been eliminated [21]. All measured XAS referred to the **E** vector parallel to the *c*-axis are shown with a correction for the geometric effect, $I_{\parallel} = \frac{4}{3}(I - \frac{1}{4}I_{\perp})$, in which I_{\perp} and I are measured XAS intensities with **E** \perp *c* and with **E** in the plane defined by the *c*-axis and the direction of incident radiation, respectively; I_{\parallel} is the deduced XAS intensity for **E** \parallel *c*.

Figure 2 presents the O 1*s* XAS of Na_{0.5}CoO₂. O 1*s* XAS measures transitions from an O 1*s* core level to unoccupied O 2*p* states mixing with bands of primary Co or Na character. One can interpret O 1*s* XAS as a one-electron addition process, i.e., $d^n \rightarrow d^{n+1}$, if the influence of the O 1*s* core hole is neglected [22, 23]. The structure in our measured XAS near the threshold arises from covalent mixing of Co 3*d* and O 2*p*; the broad feature about 540 eV corresponds to Co 4*sp* bands. The features in the region about 535 eV are attributed to transitions involv-

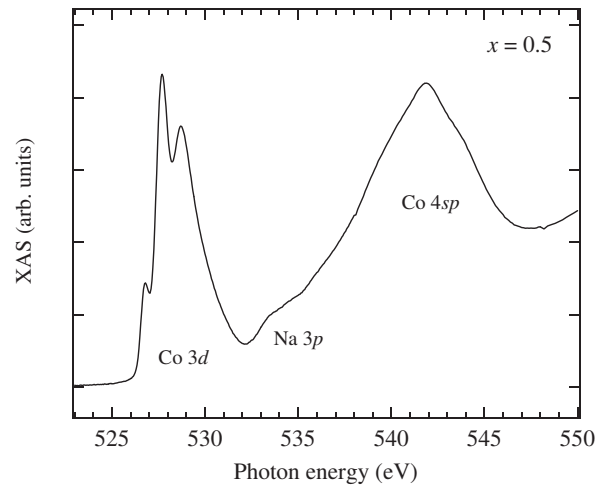


FIG. 2: O 1*s* XAS spectrum of Na_{0.5}CoO₂ measured in the total electron yield mode. The unoccupied bands with which O 2*p* states hybridize are denoted in the plot.

ing Na 3*p*. We observed three pronounced O 1*s* XAS peaks in the vicinity of the absorption threshold, implying strong hybridization between O 2*p* and Co 3*d* and many O 2*p* holes existing in Na_{0.5}CoO₂.

As for the symmetry of the pre-peaks corresponding to Co 3*d* bands, we resorted to measurements of polarization-dependent O 1*s* XAS. Figure 3 depicts O 1*s* XAS of Na_{0.5}CoO₂ with the **E** vector of photons perpendicular (I_{\perp}) and parallel (I_{\parallel}) to the crystal *c*-axis. The O 1*s* XAS shows that a peak at 526.8 eV (labelled as A) has a strong *z* component, in contrast to the in-plane orbital $d_{x^2-y^2}$ in the cuprates [24]. The ratio I_{\perp}/I_{\parallel} for peak A is 0.37 ± 0.05 , as shown in the inset of Fig. 3. The in-plane components of two other peaks at 526.8 eV and 527.6 eV (labelled as A' and B, respectively) are slightly larger than their corresponding *z* components.

The relative intensities of peaks A, A' and B in the O 1*s* XAS depend on hybridization between Co 3*d* and O 2*p*. Qualitatively, the hybridization results from the inter-atomic matrix element V_{pd} between Co 3*d* and O 2*p*, which can be expressed in terms of the Slater-Koster transfer integrals $pd\sigma$ and $pd\pi$ [25]; the ratio I_{\perp}/I_{\parallel} of O 1*s* XAS is proportional to the ratio of the averaged V_{pd}^2 with O 2*p* orbitals perpendicular and parallel to the *c*-axis. For an undistorted lattice, I_{\perp}/I_{\parallel} of O 1*s* XAS with a final state of a_{1g} symmetry is 0.25, while that of e_g symmetry is 1.0, if one uses an empirical relation $pd\sigma = -(4/\sqrt{3})pd\pi$. I_{\perp}/I_{\parallel} depends also on the distortion and the band effect. If the compressed trigonal distortion of a Na_{*x*}CoO₂ lattice is taken into account, O 1*s* XAS with final states of a_{1g} symmetry has a large out-of-plane polarization, whereas that with e_g symmetry has an in-plane polarization. Thus, our measurements that peak A and A' have opposite polarizations show that peak A results predominantly from adding an electron to

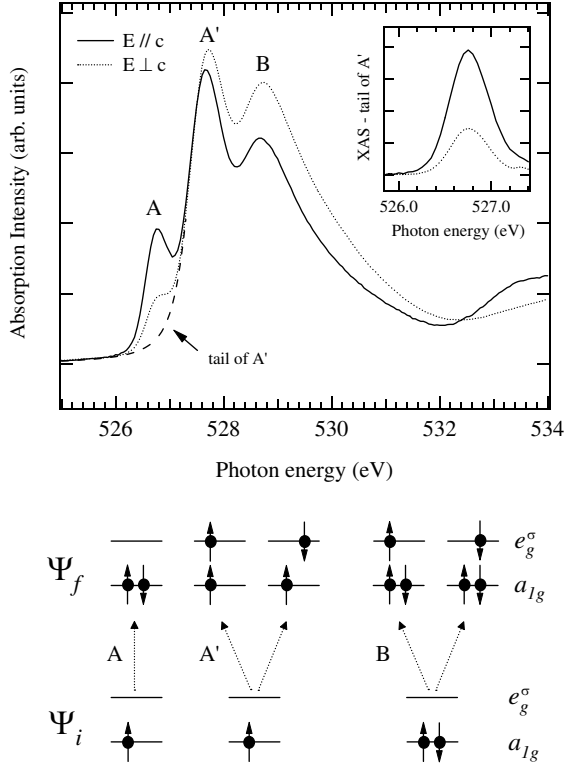


FIG. 3: Upper panel: Polarization-dependent O 1s XAS of $\text{Na}_{0.5}\text{CoO}_2$ with the \mathbf{E} vector of the light perpendicular (dotted line) and parallel (solid line) to the c -axis. The inset shows the XAS of peak A after removal of background resulting from the tail of peak A' (dashed line). Lower-panel: Energy diagrams illustrating transitions from Ψ_i in the low-spin state to Ψ_f corresponding to the symmetries of peaks A, A' and B labelled in the upper panel. The fully occupied e_g^π states are omitted from the energy diagrams for clarity.

a state of a_{1g} symmetry, whereas peaks A' and B correspond to adding electrons to states of e_g symmetry, as illustrated in the lower panel of Fig. 3. In other words, the symmetries of the transitions associated with peaks A, A' and B correspond to $(a_{1g})^1 \rightarrow (a_{1g})^2$, $(a_{1g})^1 \rightarrow (a_{1g})^1(e_g^\sigma)^1$, and $(a_{1g})^2 \rightarrow (a_{1g})^2(e_g^\sigma)^1$, respectively. Note that $(e_g^\pi)^4$ is omitted from above expressions of one-electron addition for clarity. These observations reveal that the electronic states determining the low-energy excitations of Na_xCoO_2 have predominantly a_{1g} symmetry, demonstrating that one-band models for the superconductivity of hydrated Na_xCoO_2 is a reasonable approach. Moreover, our observation of the a_{1g} symmetry of states crossing the Fermi level suggests a significant hybridization between O 2p and Co 3d, because hopping of a_{1g} states within the CoO_2 layer would be difficult without O 2p mixing. Hence, one expects that the ground-state configurations for Co^{4+} and Co^{3+} in Na_xCoO_2 have significant weights of $d^6\bar{\underline{L}}$ and $d^7\bar{\underline{L}}$, respectively, in which $\bar{\underline{L}}$ denotes an oxygen 2p hole.

To seek spectral evidence for electron correlations of 3d

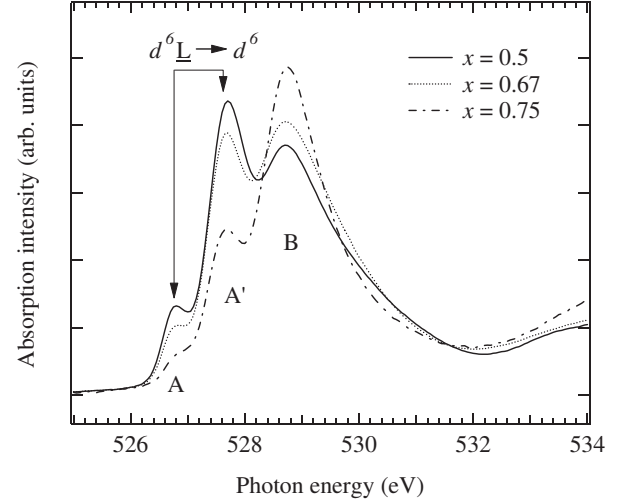


FIG. 4: Doping-dependent isotropic O 1s XAS of Na_xCoO_2 , i.e., $(I_{\parallel} + I_{\perp})/2$. The dominant transitions $d^6\bar{\underline{L}} \rightarrow d^6$ leading to the peaks A and A' are indicated in the figure.

bands, we plot doping-dependent isotropic O 1s XAS of Na_xCoO_2 in Fig. 4. The spectra are normalized to have the same intensity at 600 eV at which O 1s XAS has no doping-dependent structure. Doping of Na donates electrons to the hypothetical mother compound CoO_2 and changes a fraction x of Co^{4+} to Co^{3+} . Remarkably, we found that, as the doping x increases, the intensities of peaks A and A' decrease, but peak B increases in intensity. Thus change in the spectral weight of O 1s XAS indicates that peaks A and A' and peak B arise from transitions of adding an electron to the unoccupied states on the Co^{4+} and Co^{3+} sites, respectively. Such a spectral weight transfer is in contrast to the prediction of a one-electron theory in which a rigid-band shift is expected and the spectral weight of 3d bands is influenced only by the position of the Fermi level. The spectral-weight transfer of the one-electron addition observed in Na_xCoO_2 is a general feature of strongly correlated systems [26], as in electron-energy loss experiments [27] and O 1s XAS [28] study of $\text{La}_{2-x}\text{Sr}_x\text{CuO}_4$. Such behavior has been found in Li-doped NiO as well [29]. Both $\text{La}_{2-x}\text{Sr}_x\text{CuO}_4$ and $\text{Li}_x\text{Ni}_{1-x}\text{O}$ are charge-transfer systems; thus Na_xCoO_2 is expected to have a charge-transfer electronic structure.

We measured also Co $L_{2,3}$ -edge XAS of Na_xCoO_2 to further study its detailed electronic structure. Based on a cluster model in the CI approach [30], we simulated XAS spectra with a superposition of calculated XAS for Co^{4+} and Co^{3+} with weights of $1 - x : x$. Details of the calculations will be presented elsewhere. To summarize, the shoulder peak on the low-energy side of the L_3 edge results from the a_{1g} orbital character in the ground state. Comparing the Co L-edge XAS of $x = 0.5$, 0.67, and 0.75 with CI calculations using a series of param-

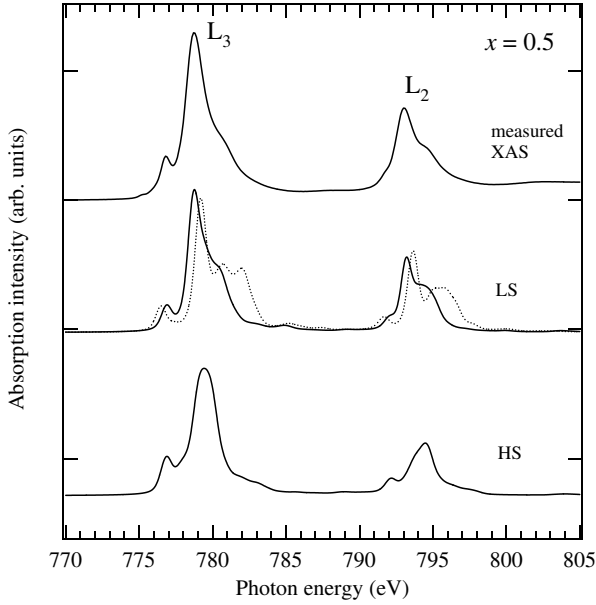


FIG. 5: Measured and calculated isotropic Co L-edge XAS of $\text{Na}_{0.5}\text{CoO}_2$. Theoretical Co L-edge XAS spectra for LS and HS Co $3d$ states were broadened with a Gaussian full width of 0.25 eV at half maximum (FWHM) and with a Lorentian FWHM of 0.2 eV. The dotted line is a simulated XAS with the parameters reported in Ref. [6].

ters, we found that the calculated XAS for Co ions in a low-spin (LS) state resembles the measured XAS satisfactorily, but the calculated XAS for high-spin (HS) ions is inconsistent with the measurement, as demonstrated in Fig. 5 for $x = 0.5$ [31]. The calculations indicate that Na_xCoO_2 has a charge-transfer energy smaller than the on-site Coulomb energy ($U_{dd}=4.5$ eV). In particular, because of the high valency, Co^{4+} ions have a negative charge-transfer energy ($\Delta \sim -1$ eV) [32], in contrast to the conclusion from the analysis of core-level photoemission data [6]. Calculations with the parameters $U_{dd}=5.5$, $\Delta=3.1$, $10Dq = 2.5$ for Co^{3+} , and $10Dq = 4.0$ for Co^{4+} , in units of eV, that Chainani *et al.* [6] concluded, give rise to a Co $2p$ XAS (dotted line in Fig. 5) inconsistent with our measurements. Thus Na_xCoO_2 exhibits a charge-transfer electronic character rather than a Mott-Hubbard character; the $d^6\bar{L}$ configuration dominates the ground state of Co^{4+} in Na_xCoO_2 [33], like Co^{4+} in SrCoO_3 [34] and $\text{La}_{1-x}\text{Sr}_x\text{CoO}_3$ [35]. These results suggest that peaks A and A' of Fig. 4 are derived from transitions of $d^6\bar{L} \rightarrow d^6$ and that the empty a_{1g} band to which the doped electrons go has predominantly O $2p$ character.

In conclusion, measurements of doping-dependent O $1s$ XAS provide a spectral fingerprint for strong correlations of $3d$ electrons in doped 2D triangular cobalt oxides. Our results reveal the charge-transfer electronic character of Na_xCoO_2 ; the doping of Na strongly affects the O $2p$ hole density. The electronic states responsible for the low-energy excitations of Na_xCoO_2 have predominantly

a_{1g} symmetry with significant O $2p$ character.

We thank F. C. Zhang, C. Y. Mou, G. Y. Guo, and L. H. Tjeng for valuable discussions. This work was supported in part by the National Science Council of Taiwan and by the MRSEC Program of the National Science Foundation of U.S. under award number DMR-02-13282.

* Corresponding author: djhuang@nsrrc.org.tw

- [1] I. Terasaki, Y. Sasago, and K. Uchinokura, Phys. Rev. B **56**, R12685 (1997).
- [2] K. Takada *et al.*, Nature **422**, 53 (2003).
- [3] R. Ray *et al.*, Phys. Rev. B **59**, 9454 (1999).
- [4] Y. Wang *et al.*, Nature **423**, 425 (2003).
- [5] T. Motohashi *et al.*, Phys. Rev. B **67**, 064406 (2003).
- [6] A. Chainani *et al.*, Phys. Rev. B **69**, 180508(R) (2004).
- [7] M. L. Foo *et al.*, Phys. Rev. Lett. **92**, 247001 (2004).
- [8] M. Z. Hasan *et al.*, Phys. Rev. Lett. **92**, 246402 (2004).
- [9] H.-B. Yang *et al.*, Phys. Rev. Lett. **92**, 246403 (2004).
- [10] D. J. Singh, Phys. Rev. B **61**, 13397 (2000).
- [11] D. J. Singh, Phys. Rev. B **68**, 020503(R) (2003).
- [12] W. Koshibae and S. Maekawa, Phys. Rev. Lett. **91**, 257003 (2003).
- [13] Y. Tanaka, Y. Yanase, and M. Ogata, cond-mat/0311266.
- [14] G. Baskaran, Phys. Rev. Lett. **91**, 097003 (2003).
- [15] Q.-H. Wang, D.-H. Lee, and P. A. Lee, Phys. Rev. B **69**, 092504 (2004).
- [16] B. Kumar and B. S. Shastry, Phys. Rev. B **68**, 104508 (2003); O. I. Motrunich and Patrick A. Lee, *ibid* **69**, 214516 (2004).
- [17] Y. Yanase, M. Mochizuki, and M. Ogata, cond-mat/0407563.
- [18] C. A. Marianetti, G. Kotliar, and G. Ceder, Phys. Rev. Lett. **92**, 196405 (2004).
- [19] L. J. Zou, J.-L. Wang, and Z. Zeng, Phys. Rev. B **69**, 132505 (2004); J. Kunes, K.-W. Lee, and W. E. Pickett, cond-mat/0308388; P. Zhang *et al.*, cond-mat/0403704.
- [20] F. C. Chou *et al.*, Phys. Rev. Lett. **92**, 157004 (2004).
- [21] D. J. Huang *et al.*, Phys. Rev. Lett. **92**, 087202 (2004).
- [22] F. M. F. de Groot *et al.*, Phys. Rev. B **40**, 5715 (1989).
- [23] J. van Elp and A. Tanaka, Phys. Rev. B **60**, 5331 (1999).
- [24] C. T. Chen *et al.*, Phys. Rev. Lett. **68**, 2543 (1992).
- [25] J. C. Slater and G. F. Koster, Phys. Rev. **94**, 1498 (1954).
- [26] H. Eskes, M. B. J. Meinders, and G. A. Sawatzky, Phys. Rev. Lett. **67**, 1035 (1991).
- [27] H. Romberg *et al.*, Phys. Rev. B **42**, 8768 (1990).
- [28] C. T. Chen *et al.*, Phys. Rev. Lett. **66**, 104 (1991).
- [29] P. Kuiper *et al.*, Phys. Rev. Lett. **62**, 221 (1989).
- [30] J. Chen *et al.*, Phys. Rev. B **69**, 085107 (2004).
- [31] Parameters (in units of eV): $U_{dd}=4.5$, $U_{dc}=5.5$, $\Delta=3.5$ (for Co^{3+}), $\Delta = -1.0$ (for Co^{4+}), $10Dq=1.5$ (for LS), $10Dq=0.5$ (for HS), $V_{eg}=3.5$, $T_{pp}=0.7$, $D_{trg} = -1.0$, and $Q_{mix} = 0.5$, where $D_{trg} \equiv E(e_g^\pi) - E(a_{1g})$; Q_{mix} is the hybridization between e_g^π and e_g^σ . See Ref. [30] for the definitions of other parameters.
- [32] Δ for Co^{4+} is defined as $E(3d^6\bar{L}) - E(3d^5)$.
- [33] The ground-state configurations for Co^{4+} are $d^5=15.9\%$, $d^6\bar{L}=48.1\%$, $d^7\bar{L}^2=31.1\%$, and $d^8\bar{L}^3=4.9\%$; those for Co^{3+} are $d^6=43.2\%$, $d^7\bar{L}=46.9\%$, and $d^8\bar{L}^2=9.9\%$.
- [34] R. H. Potze, G. A. Sawatzky, and M. Abbate, Phys. Rev. B **51**, 11501 (1995).

- [35] T. Saitoh *et al.*, Phys. Rev. B **56**, 1290 (1997).